Controllable double electromagnetically induced transparency in a closed four-level-loop cavity–atom system*

Miao-Di Guo(郭苗迪) and Xue-Mei Su(苏雪梅)†

Key Laboratory of Coherent Light, Atomic and Molecular Spectroscopy (Ministry of Education); and College of Physics, Jilin University, Changchun 130012, *China*

(Received 14 February 2017; revised manuscript received 23 March 2017; published online 25 May 2017)

We present a theoretical study of an optical cavity coupled with single four-level atoms in closed loop formed via applied control lasers. The transmitted probe field from the cavity is analyzed. We show that the electromagnetically induced transparency (EIT) in the cavity and the normal mode splitting will be very different with changing the closed interaction phase and the intensity of the free-space control laser. This coupled cavity–atom system presents a variational double-EIT that comes from modulating the splitting of the dark state, which means that we could realize the gradual transfer between one EIT peak and two EIT peaks by adjusting the applied control lasers, and the normal mode splitting sidebands will shift slightly by changing the free-space control laser. This means that we could control the output cavity probe field more freely and it is easer to realize optical switch controlled by more parameters. We also depict the angular dispersion of the intracavity probe field in different free-space control laser. The large phase shift ($-\pi \rightarrow \pi$) of the reflected intracavity probe field will be very useful for optical temporal differentiation and quantum phase gate.

Keywords: cavity quantum electrodynamics, double electromagnetically induced transparency, all optical switch, cross phase modulation

PACS: 42.50.Pq, 42.50.–p, 42.65.Pc, 42.65.–k **DOI:** 10.1088/1674-1056/26/7/074207

1. Introduction

Quantum optics studies the interactions of light and matter, no matter whether in the semiclassical method or quantum theory. An optical cavity can be used to enhance the interaction strength of matter and light, modify the rate of spontaneous radiation, and realize the reversible exchange of energy in the cavity.[1–3] It has also been used in diverse areas of research and applications such as nonlinear optical devices, quantum entanglement, and optical frequency metrology.[4–6] Extensive application of optical cavities and the studies on quantum optics and quantum electrodynamics have developed into a new research field of cavity quantum electrodynamics (cavity-QED). The interaction of two-level atoms and an optical cavity is the basic physical situation about cavity-QED first introduced by Jaynes and Cummings.[7] It is interesting to extend studies of cavity-QED to the interactions of cavity modes and multilevel atoms,[8,9] such as the intracavity electromagnetically induced transparency (EIT) in three-level or four-level atoms confined in an optical cavity, Fano-type interference in a three-level V-type atom–cavity system, and optical bistability in four-level atoms coupled with an optical cavity.[10–16]

Cavity-QED with atomic systems has been an active area of research during the last few decades. Especially the optical switch based on cavity-EIT is still a hot topic today.[17–23] Many other interesting research projects are also based on cavity-QED. For example, the internal states of an atom represent one qubit and the quantum state of the field inside the cavity represents the other in recent cavity-QED to realize implementation of a quantum phase gate,[24–27] and also the quantum networks.[28]

Here, we report a theoretical analysis of some single atoms trapped in an optical cavity, which has a closed four-level loop with three free-space lasers and an applied probe laser driving the cavity mode. This system displays varying EIT splitting and cavity normal modes shifting. We analyze the intensity ratio and phase shift of the output intracavity probe field by means of input-output theory to study how these applied free-space fields affect the double-EIT peaks and the shifting of the normal modes splitting sidebands. As a result, we find a way to realize the gradual transfer between the single-EIT peak and double-EIT peaks. We believe this work will be useful for other researchers to investigate light controlling light in a cavity and furthermore to realize much subtler all-optical switch and quantum phase gate via coupled cavity–atom systems.

This paper is organized as follows. In Section 2, we introduce our model and discuss the transmission and reflection theoretically. In Section 3, we present our numerical calculation results and make a more specific analysis. The conclusions are drawn in Section 4.

2. Theoretical analysis

The cavity–atom system is shown in Fig. 1. Some single four-level atoms are located in a single mode cavity. A probe laser injected externally from the left side of the cavity mirror

*Project supported by the National Natural Science Foundation of China (Grant No. 11174109).

†Corresponding author. E-mail: suxm@jlu.edu.cn

© 2017 Chinese Physical Society and IOP Publishing Ltd

drives the cavity mode and has a frequency detuning from the atomic transition $|1\rangle$–$|4\rangle$ by $\Delta_{\rm p}=\omega_{\rm p}-\omega_{41}$. The cavity mode is coupled to the atomic transition $|1\rangle$–$|4\rangle$ with frequency detuning $\Delta_{\rm ac}=\omega_{\rm c}-\omega_{41}$. The classical control lasers injected into the cavity perpendicularly to the propagation of the probe laser drive the atomic transitions $|2\rangle$–$|4\rangle$ and $|3\rangle$–$|4\rangle$ with Rabi frequencies Ω_1, Ω_2 and frequency detunings $\Delta_1=\omega_{1{\rm c}}-\omega_{42}$, $\Delta_2=\omega_{2{\rm c}}-\omega_{43}$, respectively, as depicted in Fig. 1. Levels $|2\rangle$ and $|3\rangle$ are coupled by a microwave laser injected by a microwave horn with Rabi frequency $\Omega_{\rm m}$ and frequency detuning $\Delta_{\rm m}=\omega_{\rm m}-\omega_{32}$. Two detectors measure the transmitted and reflected intracavity probe signals, respectively. The level configuration is also shown in Fig. 1. We choose D_2 ($5S_{1/2}\leftrightarrow 5P_{3/2}$) transitions of ^{87}Rb. Three lower states $|1\rangle$, $|2\rangle$, and $|3\rangle$ correspond to $5S_{1/2}$ ^{87}Rb $F=1$ ($m=1$), $F=1$ ($m=-1$), and $F=2$ ($m=-1$), respectively.

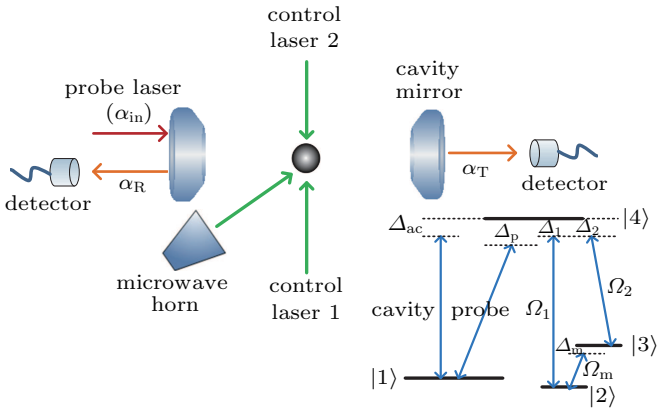


Fig. 1. (color online) Schematic diagram of the cavity–atom system and the level structure of atoms. The probe laser propagates along the axis of the cavity and the control lasers are injected into the cavity from outside.

The Hamiltonian for this coupled cavity–atom system under three-photon resonance condition ($\Delta_1=\Delta_2=\Delta_{\rm m}=0$) reads[16]

$$\begin{aligned}H=&\hbar\sum_{j=1}^{N}(\omega_{41}\sigma_{44}^{j}+\omega_{31}\sigma_{33}^{j}+\omega_{21}\sigma_{22}^{j})+\hbar\omega_{\rm c}a^{\dagger}a\\&-\hbar\sum_{j=1}^{N}(ga^{\dagger}\sigma_{14}^{j}{\rm e}^{{\rm i}\varphi_{\rm p}}+\Omega_1\sigma_{24}^{j}{\rm e}^{{\rm i}\varphi_1}\\&+\Omega_2\sigma_{34}^{j}{\rm e}^{{\rm i}\varphi_2}+\Omega_{\rm m}\sigma_{23}^{j}{\rm e}^{{\rm i}\varphi_{\rm m}})+{\rm H.C.},\end{aligned}\tag{1}$$

where φ_1, φ_2, $\varphi_{\rm m}$, and $\varphi_{\rm p}$ are the phases of the three coherent laser fields and the weak probe laser field, respectively, N is the number of atoms in the cavity, $\sigma_{mn}^{j}=|m\rangle\langle n|$ ($m,n=1,2,3,4$) is the atomic operator for the j-th atom, a ($a^{\dagger}$) is the annihilation (creation) operator of the cavity photons, $g=\mu_{14}\sqrt{\omega_{\rm c}/2\hbar\varepsilon_0 V}$ is the cavity–atom coupling coefficient, and Ω_l ($l=1,2,m$) is the Rabi frequency of the control field.

For simplicity, we consider an asymmetric Fabry–Perot cavity with field decay rates $\kappa_{\rm l}$ and $\kappa_{\rm r}$ through the left and right mirrors, respectively. The operator $a_{\rm in,l}$ ($a_{\rm in,r}$) is the field operator of an electromagnetic mode impinging from the left (right) side, while $a_{\rm out,l}$ ($a_{\rm out,r}$) describes the outgoing field to the left (right) side. We can obtain[29]

$$a_{\rm out,l}(t)+a_{\rm in,l}(t)=\sqrt{2\kappa_{\rm l}}a(t),\tag{2}$$

$$a_{\rm out,r}(t)+a_{\rm in,r}(t)=\sqrt{2\kappa_{\rm r}}a(t).\tag{3}$$

In our system, there is only one field driving the cavity mode externally from the left side of the cavity mirror. So we can calculate the reflection and transmission properties by solving the Heisenberg–Langevin equation of motion

$$\langle\dot{a}(t)\rangle=-\frac{\rm i}{\hbar}\langle[a(t),H]\rangle-\kappa\langle a(t)\rangle+\sqrt{2\kappa_{\rm l}}\langle a_{\rm in}(t)\rangle,\tag{4}$$

where κ is the total cavity field decay rate. By substituting H, the equation of motion for the expectation value of the intracavity probe field then is

$$\begin{aligned}\langle\dot{a}(t)\rangle=&-{\rm i}\omega_{\rm c}\langle a(t)\rangle+{\rm i}Ng\langle\sigma_{14}{\rm e}^{{\rm i}\varphi_{\rm p}}\rangle\\&-\kappa\langle a(t)\rangle+\sqrt{2\kappa_{\rm l}}\langle a_{\rm in}(t)\rangle.\end{aligned}\tag{5}$$

Define the Fourier components of the intracavity field by[29]

$$a(t)=\frac{1}{\sqrt{2\pi}}\int_{-\infty}^{\infty}{\rm e}^{-{\rm i}\omega(t-t_0)}a(\omega)\,{\rm d}\omega,\tag{6}$$

the intracavity probe field is derived from

$$\langle a(\omega)\rangle=\frac{\sqrt{2\kappa_{\rm l}}\langle a_{\rm in}(\omega)\rangle}{\kappa-{\rm i}\Delta_{\rm c}-{\rm i}Ng\chi},\tag{7}$$

where $\Delta_{\rm c}=\omega_{\rm p}-\omega_{\rm c}$ is the detuning of the probe laser with respect to the cavity frequency and $\chi=g[(\Delta_{\rm p}-\Delta_1)(\Delta_{\rm p}-\Delta_2)-\Omega_{\rm m}^2]/X$[30] is the atomic susceptibility in free space, with

$$\begin{aligned}X=&\Omega_1^2(\Delta_{\rm p}-\Delta_2)+\Omega_2^2(\Delta_{\rm p}-\Delta_1)\\&+\Omega_{\rm m}^2(\Delta_{\rm p}+{\rm i}\gamma_{41})-2\Omega_1\Omega_2\Omega_{\rm m}\cos(\varphi)\\&-(\Delta_{\rm p}-\Delta_1)(\Delta_{\rm p}-\Delta_2)(\Delta_{\rm p}+{\rm i}\gamma_{41}),\end{aligned}\tag{8}$$

and $\varphi=\varphi_{\rm m}+\varphi_2-\varphi_1$ being the closed interaction phase of the three coherent control lasers. Here the decay rates are given by $\gamma_{ij}=(\Gamma_i+\Gamma_j)/2$, where Γ_i is the natural decay rate of level $|i\rangle$ (with reasonable approximate definition $\Gamma_1=\Gamma_2=\Gamma_3=0$). Then it is possible for us to give the following expressions for the amplitude transmission $t(\omega)$ and reflection $r(\omega)$ coefficients:

$$t(\omega)=\frac{2\sqrt{\kappa_{\rm l}\kappa_{\rm r}}}{\kappa-{\rm i}\Delta_{\rm c}-{\rm i}Ng\chi},\tag{9}$$

$$r(\omega)=1-\frac{2\kappa_{\rm l}}{\kappa-{\rm i}\Delta_{\rm c}-{\rm i}Ng\chi}.\tag{10}$$

At the same time, the phase shifts of the transmitted and reflected fields are given by $\Phi_{\rm T}=\arg(t(\omega))$ and $\Phi_{\rm R}=\arg(r(\omega))$.

3. Numerical results

In this section, we present some numerical results to analyze the influence of the coherent control lasers on the cavity–atom system. We calculate the optical intensity ratio I_T, I_R and the optical phase shift Φ_T, Φ_R of the itracavity probe field versus probe field detuning Δ_p. For simplicity, we assume that the cavity mode is resonance with the transition $|1\rangle$–$|4\rangle$ and all results are based on full-resonance condition ($\Delta_1 = \Delta_2 = \Delta_m = 0$). We show the results in Figs. 2–5. There are four eigenstates i.e., two dressed intracavity dark states (central peaks) and two normal modes (broader sidebands).[15] When $\Omega_m = \Omega_2 = 0$, this cavity–atom system will present the typical intracavity single EIT, namely, a dark state formed with states $|1\rangle$ and $|2\rangle$ ($g\sqrt{N}|1\rangle - \Omega_1|2\rangle$). However, this dark state can be manipulated by Ω_m to create double EIT (dressed dark states). The dressed dark states consist of coherent superposition of the state $|3\rangle$ and the intracavity dark state. The two normal modes come from the vacuum Rabi splitting. They are the combination of the intracavity bright state $g\sqrt{N}|1\rangle + \Omega_1|2\rangle$ and the excited state $|4\rangle$. When there are no control lasers, the splitting of the two normal modes sidebands is $2g\sqrt{N}$. While in our system, the splitting is $2\sqrt{\Omega_1^2 + \Omega_m^2 + g^2N + \frac{\Omega_2}{2}(|\sin\frac{\varphi}{2}| - |\cos\frac{\varphi}{2}|)}$. The second term in the above formula comes from the nonzero closed interaction phase and the third control laser Ω_2. It is different from Ref. [15], we care about how Ω_2 and another factor φ affect these dressed intracavity dark states and the coupled cavity–atom normal modes.

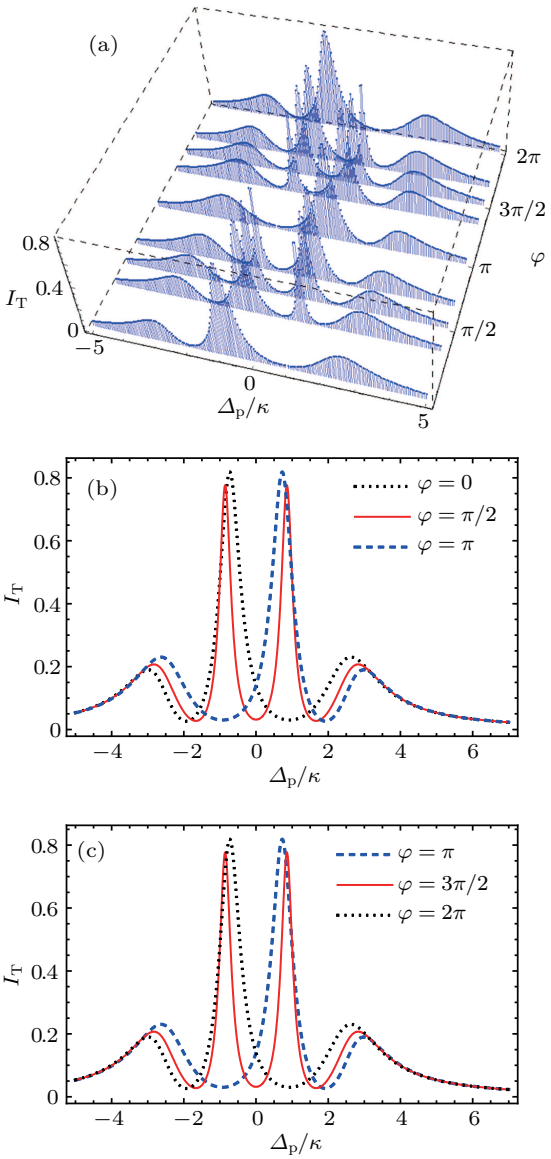


Fig. 2. (color online) (a) The intensity ratio of the transmitted probe field versus the probe frequency detuning Δ_p/κ in different closed interaction phases. Panels (b) and (c) show the results of $\varphi = 0$, $\pi/2$, π and $\varphi = \pi$, $3\pi/2$, 2π, respectively.

Figure 2 shows the transmission spectra in different closed interaction phases φ when $\Omega_1 = \Omega_2 = \Omega_m = \kappa$ and the other parameters are $g = 1.5\kappa$, $N = 2$, $\kappa_l = 0.6\kappa$, $\kappa_r = 0.4\kappa$, and $\kappa = \gamma_{41}$. From Fig. 2(a), we can see that the transmission spectra are symmetrical about plane $\varphi = \pi$. This is shown more obviously in Figs. 2(b) and 2(c). When the closed interaction phase is changed discretely from 0 to π in Fig. 2(b), we find that the EIT peak changes from one in the position of negative frequency detuning to the symmetrical splitting double-EIT peaks and then to one peak again while at positive frequency detuning. However, things are reversed when φ is altered from π to 2π discontinuously in Fig. 2(c). Indeed, this phenomenon is not only presented in the intracavity dark states, but also for the splitting normal modes. As we can see, the position of the normal mode sidebands will also change with varying closed interaction phase φ, and $\varphi = \pi$ is also the plane of symmetry. Therefore, it is only necessary for us to explore the transmitted probe field with φ changing from 0 to π. Here we obtain the eigenvalues of double-EIT as

$$\lambda_l = -\left(\Omega_m - \Omega_2\left|\sin\frac{\varphi}{2}\right|^4 + \frac{\Omega_2}{3}\left|\sin\varphi\right|\right) \times \sqrt{g^2N/\left(\Omega_1^2 + \Omega_m^2 + g^2N + 2\Omega_2^2\left|\cos\frac{\varphi}{2}\right|^2\right)}, \quad (11)$$

$$\lambda_r = -\left(\Omega_m - \Omega_2\left|\cos\frac{\varphi}{2}\right|^4 + \frac{\Omega_2}{3}\left|\sin\varphi\right|\right) \times \sqrt{g^2N/\left(\Omega_1^2 + \Omega_m^2 + g^2N + 2\Omega_2^2\left|\cos\frac{\varphi}{2}\right|^2\right)}, \quad (12)$$

which is consistent with the spectra derived from the input-output theory.

Figure 3 depicts the transmitted spectra of the intracavity probe field with varying Ω_2 from 0 to κ discretely at $\varphi = 0$, $\pi/2$, and π, respectively. As we can see, when $\Omega_2 = 0$ (the black dotted lines in Fig. 3), the shape of transmission is always symmetrical about line $\Delta_p = 0$ no matter what the closed interaction phase φ is. This can be explained by a simple four-level atom–cavity model. We all know that this system

can degenerate to a three-level Λ-type cavity-EIT configuration when $\Omega_2 = \Omega_m = 0$.[11] We have also verified it in our analysis formulas. When $\Omega_m \neq 0$, the central EIT peak is split into two peaks symmetrically and the peaks separation is approximately equal to $2\Omega_m$.[15] However, when we apply another coherent control laser Ω_2, namely, $\Omega_m \neq 0$ and $\Omega_2 \neq 0$, it will destroy the manipulation of Ω_m on the coherent superposition of cavity-EIT (intracavity dark state) and the atomic state $|3\rangle$ and also on the two normal modes. For example, in Fig. 3(a), the spectrum features four symmetrical peaks when $\Omega_2 = 0$ (black dotted line), with Ω_2 increasing to 0.5κ, the symmetrical splitting of the dark state is broken. When Ω_2 is equal to Ω_m ($\Omega_2 = \Omega_m = \kappa$), the double EIT peaks will become a single peak at the position of frequency detuning $\Delta_p/\kappa = -\Omega_m\sqrt{g^2N/(\Omega_1^2+\Omega_m^2+g^2N+2\Omega_2^2)}$, and the principle is similar to the situation in Fig. 3(c) except that the single peak will be at the position of frequency detuning $\Delta_p/\kappa = \Omega_m\sqrt{g^2N/(\Omega_1^2+\Omega_m^2+g^2N+2\Omega_2^2)}$. In Fig. 3(b), the central peaks are a little different from those in Figs. 3(a) and 3(c). As it is shown to us, whatever the control Rabi frequency Ω_2 is, there will always be two peaks symmetrical about line $\Delta_p = 0$. This can be explained by Eqs. (11) and (12) with $\varphi = \pi/2$.

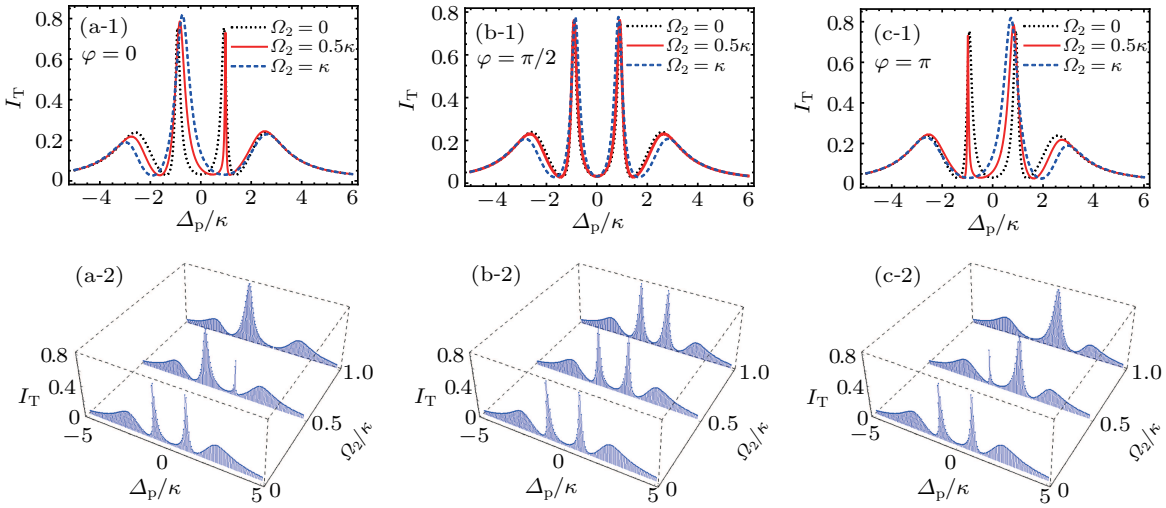


Fig. 3. (color online) The intensity ratio of the transmitted probe field versus the probe frequency detuning for (a) $\varphi = 0$, (b) $\varphi = \pi/2$, (c) $\varphi = \pi$. The parameters used here are $g = 1.5\kappa$, $N = 2$, $\kappa_l = 0.6\kappa$, $\kappa_r = 0.4\kappa$, $\kappa = \gamma_{41}$, $\Omega_1 = \Omega_m = \kappa$, and $\Omega_2 = 0, 0.5\kappa, \kappa$.

As we have mentioned before, the coherent control laser Ω_2 will also influence the normal modes. In Fig. 2(b), we can see that the normal modes shift with varying φ and the two normal modes are symmetrical about line $\Delta_p = 0$ only when $\varphi = \pi/2$. In Figs. 3(a)–3(c), we can also find the shifting of the normal modes with varying intensity of control Rabi frequency Ω_2. The peak shifting of the normal modes approximately satisfies the following expression:

$$\lambda_{nl} = -\sqrt{\Omega_1^2+\Omega_m^2+g^2N} - \frac{\Omega_2}{2}\left|\cos\frac{\varphi}{2}\right|, \tag{13}$$

$$\lambda_{nr} = \sqrt{\Omega_1^2+\Omega_m^2+g^2N} + \frac{\Omega_2}{2}\left|\sin\frac{\varphi}{2}\right|, \tag{14}$$

which is also consistent with the spectra in Figs. 2 and 3.

We also analyze the reflected intracavity probe field, as shown in Fig. 4, on which the influence of the control laser is the same as the transmitted intracavity probe field. For simplicity but to be clear, we only show the reflected intensity ratio I_R with different φ when $\Omega_2 = \kappa$ and with different control Rabi frequencies Ω_2 when $\varphi = \pi/2$. The parameters used in Figs. 4(a) and 4(b) are the same as those used in Figs. 2 and 3, respectively.

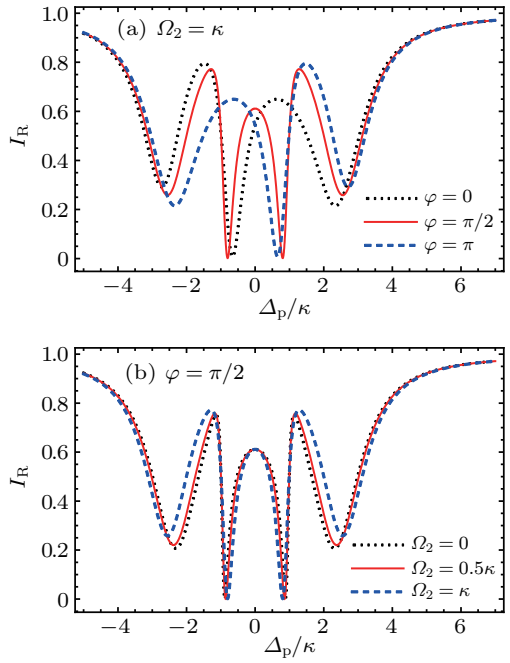


Fig. 4. (color online) Reflected spectra of intracavity probe field (a) with different closed interaction phases when $\Omega_2 = \kappa$ and (b) with different control Rabi frequencies when $\varphi = \pi/2$.

Besides the intensity ratio of the intracavity probe field, we care about the phase shift of the intracavity probe field as well. Therefore, in Figs. 5 and 6, we show how the closed interaction phase φ and the strength of the coherent control laser Ω_2 affect the angular dispersions of the transmitted and reflected intracavity probe fields. As depicted, the phase shift of both transmitted and reflected intracavity probe fields can be controlled by adjusting the closed interaction phase φ. Especially for the reflected spectra in Fig. 5(b), they present sharp abnormal angular dispersions at the EIT peaks, which means that we can realize large cross phase modulation (XPM) ($-\pi \rightarrow \pi$) with low intensity control laser.[31] Moreover, the reflected spectra have sharper slopes comparing with the transmitted spectra from Figs. 5(a) and 5(b). To explain the difference between the reflected and transmitted dispersions, we draw the phase curves at three situations: $\kappa_{\rm l} = 0.6\kappa$, 0.5κ, 0.4κ ($\kappa_{\rm r} = 0.4\kappa, 0.5\kappa, 0.6\kappa$), where the strength of the probe field injected into the cavity increases with $\kappa_{\rm l}$ increasing. As shown in Figs. 5(a), 5(c), and 5(e), the dispersions of the transmitted spectra at EIT resonance keep almost the same at the three situations. This shows that the intracavity field distribution keeps the same with different $\kappa_{\rm l}$ ($0.6\kappa, 0.5\kappa, 0.4\kappa$). However, the phase of the reflected spectra is decided by the difference between the distribution of intracavity field and that of atomic absorption (Eq. (10)) and on the other hand, the larger abnormal dispersion is obtained at EIT windows[31] when the interaction strength is enlarged. So the dispersion of the reflected field increases with $\kappa_{\rm l}$ increasing and even has a very sharp slope in contrast to the transmitted field. According to these analyses, our system with large $\kappa_{\rm l}$ is advantageous to obtaining a large phase shift of the reflected spectra.

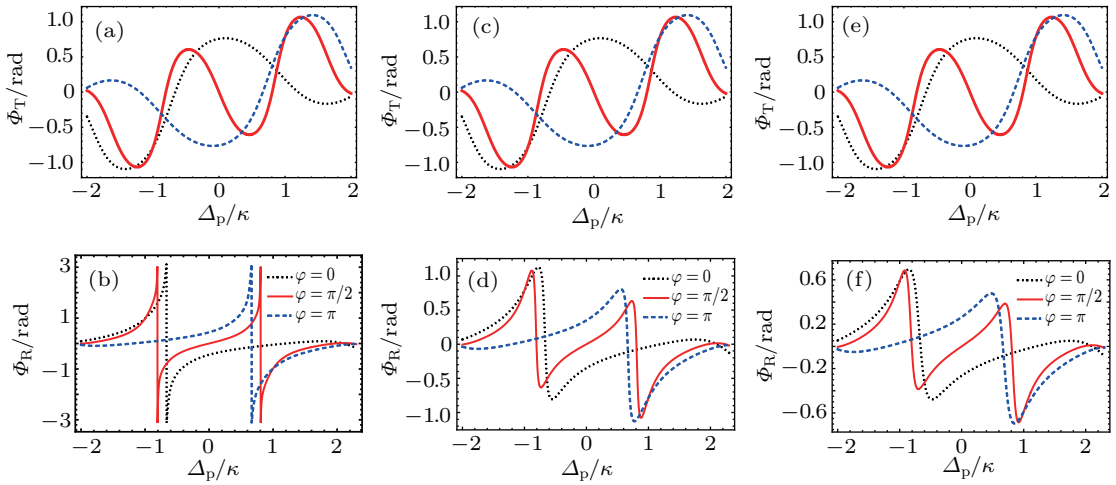


Fig. 5. (color online) The phase shift of (a), (c), (e) the transmitted probe field and (b), (d), (f) the reflected probe field versus probe frequency detuning $\Delta_{\rm p}/\kappa$: (a), (b) $\kappa_{\rm l} = 0.6\kappa$, $\kappa_{\rm r} = 0.4\kappa$; (c), (d) $\kappa_{\rm l} = 0.5\kappa$, $\kappa_{\rm r} = 0.5\kappa$; (e), (f) $\kappa_{\rm l} = 0.4\kappa$, $\kappa_{\rm r} = 0.6\kappa$. The other parameters are $g = 1.5\kappa$, $N = 2$, $\kappa = \gamma_{41}$, $\Omega_1 = \Omega_2 = \Omega_{\rm m} = \kappa$, $\varphi = 0$, $\pi/2$, and π.

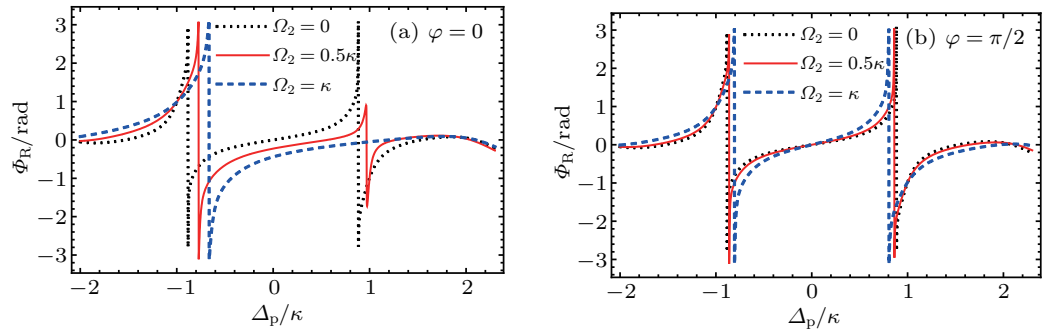


Fig. 6. (color online) The phase shift of the reflected probe field versus probe frequency detuning $\Delta_{\rm p}/\kappa$ for (a) $\varphi = 0$ and (b) $\varphi = \pi/2$. The parameters are $g = 1.5\kappa$, $N = 2$, $\kappa_{\rm l} = 0.6\kappa$, $\kappa_{\rm r} = 0.4\kappa$, $\kappa = \gamma_{41}$, $\Omega_1 = \Omega_{\rm m} = \kappa$, $\Omega_2 = 0, 0.5\kappa, \kappa$.

When we make the closed interaction phase $\varphi = 0$, the asymmetry on the phase shift of the double-EIT peaks is derived from free space control laser (control Rabi frequency Ω_2) as shown in Fig. 6(a). While $\varphi = \pi/2$, the angular dispersion at double EIT peaks is always symmetrical as shown in Fig. 6(b). That is reasonable, since the real part of the susceptibility can be simplified as

$$\mathrm{Re}[\chi]=\begin{cases}-\dfrac{g(\Delta_{\mathrm{p}}^2-\Omega_{\mathrm{m}}^2)[\Delta_{\mathrm{p}}^3+2\Omega_1\Omega_2\Omega_{\mathrm{m}}-\Delta_{\mathrm{p}}(\Omega_1^2+\Omega_2^2+\Omega_{\mathrm{m}}^2)]}{\gamma_{41}^2(\Delta_{\mathrm{p}}^2-\Omega_{\mathrm{m}}^2)^2+[\Delta_{\mathrm{p}}^3+2\Omega_1\Omega_2\Omega_{\mathrm{m}}-\Delta_{\mathrm{p}}(\Omega_1^2+\Omega_2^2+\Omega_{\mathrm{m}}^2)]^2}, & \varphi=0,\\ -\dfrac{g\Delta_{\mathrm{p}}(\Delta_{\mathrm{p}}^2-\Omega_{\mathrm{m}}^2)(\Delta_{\mathrm{p}}^2-\Omega_1^2-\Omega_2^2-\Omega_{\mathrm{m}}^2)}{\gamma_{41}^2(\Delta_{\mathrm{p}}^2-\Omega_{\mathrm{m}}^2)^2+\Delta_{\mathrm{p}}^2(\Delta_{\mathrm{p}}^2-\Omega_1^2-\Omega_2^2-\Omega_{\mathrm{m}}^2)^2}, & \varphi=\pi/2,\end{cases} \tag{15}$$

namely, there is always $|\mathrm{Re}[\chi(\Delta_{\mathrm{p}})]|=|\mathrm{Re}[\chi(-\Delta_{\mathrm{p}})]|$ when $\varphi=\pi/2$.

It is clear that the evolution of the double intracavity EIT can be manipulated flexibly by either the intensity or the closed interaction phase of the control lasers.

4. Conclusion

We study a cavity–atom system which consisted of some single four-level atoms coupled with an asymmetrical cavity. By applying the third coherent control laser Ω_2, this system contains a closed interaction phase φ that can modify the transmitted and reflected intracavity probe fields, namely, besides the strength of the control Rabi frequency, there is also another factor that can influence the EIT peaks and the normal modes. We specifically analyze the changing of this kind of double-EIT peaks and the shifting of the cavity normal modes depending on the closed interaction phase and strength of the control lasers. Therefore, it enables us to control the cavity EIT to realize a gradual transfer between single intracavity EIT and double intracavity EIT via changing either the signal intensity or the closed interaction phase. The large XPM ($-\pi\rightarrow\pi$) in our system could be useful for quantum phase gate and all-optical temporal differentiation.[32]

References

[1] Haroche S and Kleppner D 1989 *Physics Today* **42** 0124
[2] Eberly J H, Narozhny N B and Sanchez-Mondragon J J 1980 *Phys. Rev. Lett.* **44** 1323
[3] Zou H M and Fang M F 2016 *Chin. Phys. B* **25** 070305
[4] Marbuger J H and Fellber F S 1978 *Phys. Rev. A* **17** 335
[5] Nihira H and Stroud C R Jr 2009 *Phys. Rev. A* **80** 042329
[6] Tuchman A K, Long R, Vrijsen G, Boudet J, Lee J and Kasevich M A 2006 *Phys. Rev. A* **74** 053821
[7] Jaynes E T and Cummings F W 1963 *Proc. IEEE* **51** 89
[8] Xue Y L, Zhang K, Feng B H and Li Z Y 2016 *Chin. Phys. Lett.* **33** 074204
[9] Hai L, Tan L, Feng J S, Xu W B and Wang B 2014 *Chin. Phys. B* **23** 024202
[10] Lukin M D, Fleischhauer M, Scully M O and Velichansky V L 1998 *Opt. Lett.* **23** 295
[11] Mücke M, Figueroa E, Bochmann J, Hahn C, Murr K, Ritter S, Villas-Boas C J and Rempe G 2010 *Nature* **465** 755
[12] Wang H, Goorskey D J, Burkett W H and Xiao M 2000 *Opt. Lett.* **25** 1732
[13] Wu H B, Gea-Banacloche J and Xiao M 2008 *Phys. Rev. Lett.* **100** 173602
[14] Cheng Y, Tan Z, Wang J, Zhu Y F and Zhan M S 2016 *Chin. Phys. Lett.* **33** 014202
[15] Wang Y H, Zhang J P and Zhu Y F 2012 *Phys. Rev. A* **85** 013814
[16] Sawant R and Rangwala S A 2016 *Phys. Rev. A* **93** 023806
[17] Wei X G, Zhang J P and Zhu Y F 2010 *Phys. Rev. A* **82** 033808
[18] Nielsen A E B and Kerckhoff J 2011 *Phys. Rev. A* **84** 043821
[19] Xu J P, Al-Amri M, Yang Y P, Zhu S Y and Zubairy M S 2012 *Phys. Rev. A* **86** 033828
[20] Zou B C, Tan Z, Musa M and Zhu Y F 2014 *Phys. Rev. A* **89** 023806
[21] Peng Y D, Niu Y P, Yang A H, Li D H, Liang M and Gong S Q 2014 *Opt. Commun.* **313** 416
[22] Zhang X, Li R and Wu H B 2016 *Nature* **6** 22560
[23] Li N, Xu J P, Song G, Zhu C J, Xie S Y, Yang Y P, Zubairy M S and Zhu S Y 2016 *Phys. Rev. A* **93** 043819
[24] Zubairy M S, Kim M and Scully M O 2003 *Phys. Rev. A* **68** 033820
[25] Chen C Y, Feng M and Gao K L 2006 *Phys. Rev. A* **73** 064304
[26] Rauschenbeutel A, Nogues G, Osnaghi S, Bertet P, Brune M, Raimond J M and Haroche S 1999 *Phys. Rev. Lett.* **83** 5166
[27] Tang S Q, Zhang D Y, Wang X W, Xie L J and Gao F 2011 *Chin. Phys. B* **20** 040308
[28] Reiserer A and Rempe G 2015 *Rev. Mod. Phys.* **87** 1379
[29] Walls D F and Milburn G J 2007 *Quantum Optics* (Berlin: Springer) pp. 127–133
[30] Xue Y, Wang G, Wu J H, Xu W H, Wang H H, Gao J Y and Babin S A 2004 *Phys. Lett. A* **324** 388
[31] Zou B C and Zhu Y F 2013 *Phys. Rev. A* **87** 053802
[32] Berger N K, Levit B, Fischer B, Kulishov M, Plant D V and Azaña J 2007 *Opt. Express* **15** 371